MIT Open Access Articles

Cavity-enhanced multispectral photodetector using phase-tuned propagation: theory and design

Massachusetts Institute of Technology

Cavity-enhanced multispectral photodetector using phase-tuned propagation: theory and design

Jianfei Wang, Juejun Hu,* Xiaochen Sun, Anu Agarwal, and Lionel C. Kimerling

Microphotonics Center, Massachusetts Institute of Technology, Cambridge, Massachusetts 02139, USA
*Corresponding author: hujuejun@mit.edu

We propose and theoretically analyze what we believe to be a novel design of cavity-enhanced photodetectors capable of sensing multiple wavelengths simultaneously in a *single* pixel. The design is based on phase-tuned propagation of resonant modes in cascaded planar resonant cavities. We show that this concept can be generalized to detect multiple wavelength combinations covering the entire near to far infrared spectrum. Besides its multispectral detection capability, the design also features minimal spectral cross talk and significantly suppressed noise. The intrinsic design versatility and scalability, as well as process compatibility with planar microfabrication, suggest the design's wide application potential for telecommunications, infrared imaging, and biochemical sensing. © 2010 Optical Society of America

OCIS codes: 310.6805, 040.5160, 110.4234, 040.3060.

Multispectral infrared (IR) detection has been widely employed for applications including hyperspectral imaging, IR spectroscopy, and target identification. Traditional multispectral technology is based on the combination of single spectral focal plane arrays (FPAs) and spectral filters or spectrometers, which require bulky high-cost mechanical scanning instruments and have a slow response. Single pixels capable of detecting multiple wavebands simultaneously thus have become the focus of the third generation FPA development [1]. Recently, three-color HgCdTe photodiodes have been demonstrated, although their spectral cross talk is large (>10%) [2]. A competing multicolor detector technology is quantum-well IR photodetectors (QWIPs) [1]. However, the QWIP device optimization is limited by its low quantum efficiency (QE) (<10%) [3]. Other alternative solution tandem detectors have limited band selection options and large cross talks due to material compatibility issues and radiative coupling. A solution, which combines a high QE and a low spectral cross talk, is yet to be explored.

Our approach involves a multilayer cascaded cavity structure shown schematically in Fig. 1. Each wavelength to be detected leads to a unique resonant mode locally confined within one cavity, where an absorbing active layer is placed for spectral selective detection of this wavelength. The major challenge is the spatial localization of the resonant modes without compromising the QE. Our solution employs a novel phase-tuned propagation design. We insert phase-tuning layers between the cascaded cavities to control the optical phase and hence the coupling strength between the incident light and the resonant modes. Thereby, we show that near unity QEs can be achieved for all cavities. Comparing to previous work on multispectral detection using a single cavity [4], spectral cross talk is significantly suppressed given the wavelength-selective spatial localization of resonant modes in different cavities. The electrical signal originating from each wavelength may be separately read out by contacting the corresponding active layer, either in a photoconductive [4] or in a photovoltaic

mode. Further, since resonant cavity enhancement effect leads to field buildup in the cavity and dramatically increases absorption, IR active layers with reduced thicknesses can be used while maintaining near-unity QEs. Consequently, detector noise can be suppressed without compromising responsivity. In this Letter, we theoretically analyze the design principles of the multispectral pixel design using the transfer matrix method (TMM).

To start with, we consider an IR active layer sandwiched within a generic multilayer resonant cavity stack, where near-unity IR absorption (internal QE) can be attained when the critical coupling condition is met at the resonant wavelength,

$$R_t = (1 - A_L)R_b, \quad R_b \to 1, \tag{1}$$

where R_t and R_b are the reflectivities of top and bottom mirrors and A_L denotes the optical resonant mode loss. When the cavity quality factor $Q \gg 1$, A_L can be calculated using cavity perturbation theory as

$$A_L = \varepsilon d \frac{\displaystyle\int_{\text{active}} \alpha |E_0|^2 dV}{\displaystyle\int_{\text{stack}} \varepsilon_c |E_0|^2 dV}, \tag{2}$$
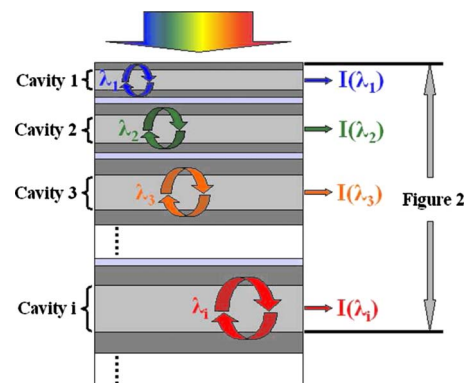

Fig. 1. (Color online) Cross sectional schematic of a multispectral pixel consisting of cascaded planar resonant cavities (not drawn to scale).

where ε and α are the dielectric constant and the absorption coefficient of the IR active material, d is the cavity length, E_0 denotes the electric field distribution of the resonant mode, and ε_c gives the dielectric constant profile of the stack. Notably, when the active material completely fills the cavity between the two mirrors, A_L can be given as $(1-e^{-2\alpha d})$ and Eq. (1) reduces to the critical coupling formulation by Unlu and Strite [5]. Equation (1) states that given a bottom mirror with near unity reflectivity $(R_b \rightarrow 1)$, the maximum QE at the resonant wavelength may be obtained by choosing a top mirror reflectivity (R_t) to satisfy Eq. (1).

Now we apply the above analysis to the ith ($i = 1, 2, 3, \dots$) cavity in Fig. 1. As shown in Fig. 2, the "top mirror" of the ith cavity includes cavities 1 to $i - 1$. To satisfy Eq. (1), we insert a coupling-matching layer m in the top mirror stack to allow effective tuning of the top mirror reflectivity $R_{t,i}$ (the second subscript i denotes the sequential number of cavity in the stack).

Here we use TMM to derive the top mirror reflectivity $R_{t,i}$ of the ith cavity as shown in Fig. 2. Following the convention of Sun [6], we label the layers sequentially starting from the incident medium. The transfer matrix T_f of the entire stack may be written as

$$T_f = T_{(3)} M_1^{-1} M_m L_m T_{(2)}, \qquad (3)$$

where $T_{(2)}$ corresponds to the transfer matrix of layers from the first to the $(i-1)$th cavity including the mth coupling-matching layer and $T_{(3)}$ is the transfer
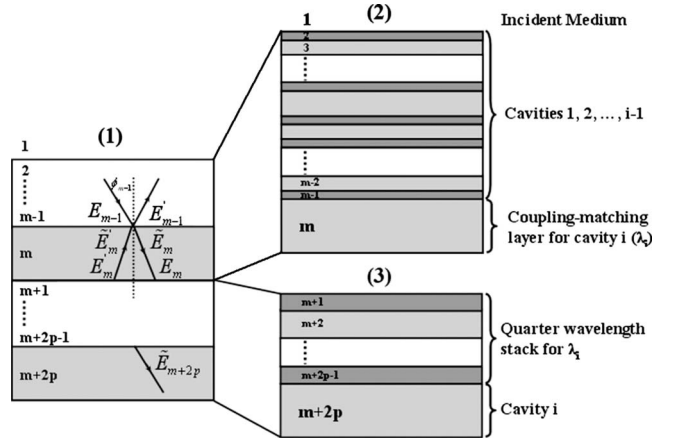

Fig. 2. Structures used in deriving the coupling-matching condition for cavity i. Stack (1) is the entire structure which can be decomposed into stacks (2) and (3). The layers corresponding to stack (1) are also shown in Fig. 1.

matrix of the quarter-wavelength stack (QWS) designed for the ith cavity's resonant wavelength λ_i. It can be proven that the matrix $T_{(2)}$ may be generically represented as

$$T_{(2)} = M_m^{-1}(M_{m-1}L_{m-1}M_{m-1}^{-1}) \cdots (M_2 L_2 M_2^{-1}) M_1$$
$$= \begin{pmatrix} T_{(2)22} e^{-i\theta_{22}} & T_{(2)21} e^{-i\theta_{21}} \\ T_{(2)21} e^{i\theta_{21}} & T_{(2)22} e^{i\theta_{22}} \end{pmatrix}, \qquad (4)$$

where $T_{(2)21}$, $T_{(2)22}$, θ_{21}, and θ_{22} are functions of ϕ_j, n_j, μ_j, t_j ($j = 1$ to m), and λ. In high-index-contrast Bragg cavities, the angular dependence of spectral response is minimal. Practically we only need to consider normal incidence. $T_{(3)}$ then follows ($\lambda = \lambda_i$, p pairs)

$$T_{(3)} = M_{m+2p}^{-1}(M_{m+2p-1}L_{m+2p-1}M_{m+2p-1}^{-1}) \cdots (M_{m+1}L_{m+1}M_{m+1}^{-1})M_1 = (i)^{2p-1}\begin{pmatrix} A+B & -A+B \\ A-B & -A-B \end{pmatrix}, \qquad (5)$$

where

$$A = \frac{n_1}{2n_{m+2p-1}}\left(\frac{n_{m+2}}{n_{m+1}}\right)^{p-1}, \quad B = \frac{n_{m+2p-1}}{2n_{m+2p}}\left(\frac{n_{m+1}}{n_{m+2}}\right)^{p-1}. \qquad (6)$$

Substituting Eqs. (7) and (8) into Eq. (6), we have

$$R_{t,i} = |r|^2 = \left| -\frac{T_{f21}}{T_{f22}} \right|^2 = \left| \frac{A n_m(T_{(2)21}e^{i(\theta_{21}+\theta_{22})} - T_{(2)22}e^{2i\delta_m}) + B n_1(T_{(2)21}e^{i(\theta_{21}+\theta_{22})} + T_{(2)22}e^{2i\delta_m})}{A n_m(T_{(2)22}e^{i(\theta_{21}+\theta_{22})} - T_{(2)21}e^{2i\delta_m}) + B n_1(T_{(2)22}e^{i(\theta_{21}+\theta_{22})} + T_{(2)21}e^{2i\delta_m})} \right|^2, \qquad (7)$$

where $\delta_m = (2\pi/\lambda_i)n_m t_m$, and n_m and t_m are the refractive index and the thickness of the mth layer, i.e., the coupling-matching layer at λ_i. Such a functional dependence provides a lever to tune $R_{t,i}$ simply by adjusting t_m to satisfy Eq. (1) and thereby reach a near unity QE. In the example we give later, we illustrate how this condition can be solved graphically.

There are two special cases though where the $R_{t,i}$ tuning mechanism fails. When the resonant wavelength of the ith cavity λ_i falls in one of the stop bands of cavities 1 to $i - 1$, $R_{(2)} \sim 1$ and $|T_{(2)21}|$

$\approx |T_{(2)22}|$. Equation (7) then reduces to $R_{t,i} \approx 1$ regardless of the value of t_m. In the second case, λ_i coincides with the reflectivity minimum of ripples outside the photonic stop bands of cavities 1 to $i - 1$ and $R_{(2)} \sim 0$. In this case, $R_{t,i} \approx |(A n_m - B n_1)/(A n_m + B n_1)|$, independent on t_m. Both cases can be avoided by properly choosing the refractive index contrast of mirror materials in cavities 1 to i.

To summarize, we can follow the generic procedures to design multispectral detectors for selectively detecting N different wavelengths $\lambda_1, \lambda_2, \dots, \lambda_N$:

(1) Select mirror materials for the N wavelengths to avoid overlapping λ_i and the photonic stop bands of cavities 1 to $i-1$, and to minimize parasitic loss due to mirror absorption.

(2) Start from the first cavity on top of the stack and choose appropriate numbers of top/bottom mirror QWS pairs to satisfy Eq. (1).

(3) Move on to the next cavity i and adjust the coupling-matching layer thickness sandwiched between cavity $i-1$ and cavity i so that the critical coupling condition is met.

(4) Repeat steps (2) and (3) until the entire stack design is complete.

As an example to validate the principles, $\lambda_1 = 1550$ nm and $\lambda_2 = 3600$ nm are chosen as the two wavelengths to be detected. As_2S_3 and a-Ge are used as the mirror materials given their IR transparency. PbTe layers are used as IR absorbers in both cavities. The wavelength-dependent refractive indices are measured using IR ellipsometry [7].

Figure 3(a) shows a schematic cross section of the pixel designed following the above procedures, and Fig. 3(b) illustrates graphic solutions to the critical coupling condition (1). Here we use a 340-nm-thick Ge layer between the two cavities as the coupling-matching layer (pair No.=2). Figure 3(c) shows the QE spectra for the two PbTe absorbers. The peak QE over 80% is realized in both wavebands with only 50 and 100 nm thick PbTe absorbers given the strong resonant cavity enhancement. In comparison, a conventional free-space PbTe detector operating at 3600

nm wavelength requires an absorber as thick as 10 μm. Consequently, the G-R and Johnson noise in our design will be ten times lower, since both types of noise scale with the square root of the active material volume. The ripples between peaks (side lobes) can be suppressed by integrating a planar band-stop filter or employing an apodized cavity design.

Besides the high QE, the high degree of spatial localization of modes effectively minimizes the spectral cross talk. Figure 3(d) plots the light intensity distributions in the stack at the two resonant wavelengths. The spectral cross talk in a dual wavelength detector can be measured using [8]

$$\text{Cross talk} = \frac{\eta_{\text{active2}}(\lambda_1)}{\eta_{\text{active2}}(\lambda_2)}, \quad \lambda_1 < \lambda_2, \qquad (8)$$

where $\eta_{\text{active2}}(\lambda_1)$ is the QE of the second active layer at λ_1, and $\eta_{\text{active2}}(\lambda_2)$ is the peak QE of the second active layer at λ_2. Our design gives a spectral cross talk as low as 0.1%, more than 2 orders of magnitude lower compared to a tandem design [8] or a single cavity design [4].

To summarize, we propose and analyze a versatile and scalable design for cavity-enhanced photodetectors capable of sensing multiple wavebands simultaneously in a single pixel. The design is based on phase-tuned propagation in cascaded planar resonant cavities and this concept can be generalized to detect virtually any arbitrary number of wavelengths. This proposed pixel structure combines a high QE, reduced detector noise, as well as a low cross talk, and thus may find wide applications in security surveillance, imaging, and spectroscopy.
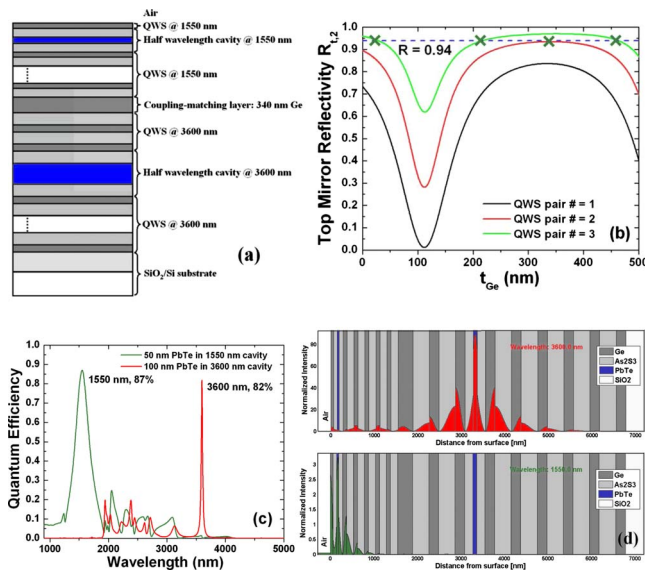
Fig. 3. (Color online) (a) Schematic cross section of the pixel designed to detect 1550 and 3600 nm wavelengths simultaneously. (b) Solid curves: $R_{t,2}$ as a function of coupling-matching layer's thickness for different QWS pair numbers; dashed line: reflectivity corresponding to the critical coupling condition (1); green crosses: thickness values at which the critical coupling condition is met. (c) QE spectra calculated for two PbTe absorbers in the two cascaded resonant cavities, showing two detection bands peaked at 1550 and 3600 nm with high QE and low spectral cross talk. (d) Normalized light intensity spatial distribution for 3600 and 1550 nm wavelengths, illustrating high degree of modal spatial localization.

References

1. A. Rogalski, J. Antoszewski, and L. Faraone, J. Appl. Phys. **105**, 091101 (2009).
2. L. G. Hipwood, C. L. Jones, C. D. Maxey, H. W. Lau, J. Fitzmaurice, R. A. Catchpole, and M. Ordish, Proc. SPIE **6206**, 620612 (2006).
3. S. D. Gunapala, S. V. Bandara, J. K. Liu, J. M. Mumolo, C. J. Hill, S. B. Rafol, D. Salazar, J. Woollaway, P. D. LeVan, and M. Z. Tidrow, Infrared Phys. Technol. **50**, 217 (2007).
4. X. C. Sun, J. J. Hu, C. Y. Hong, J. F. Viens, X. M. Duan, R. Das, A. M. Agarwal, and L. C. Kimerling, Appl. Phys. Lett. **89**, 223522 (2006).
5. M. S. Unlu and S. Strite, J. Appl. Phys. **78**, 607 (1995).
6. X. C. Sun, "Ge-on-Si light-emitting materials and devices for silicon photonics," Ph.D. dissertation (MIT, 2009).
7. J. Wang, J. Hu, X. Sun, A. M. Agarwal, L. C. Kimerling, D. R. Lim, and R. A. Synowicki, J. Appl. Phys. **104**, 053707 (2008).
8. R. A. Coussa, A. M. Gallagher, K. Kosai, L. T. Pham, G. K. Pierce, E. P. Smith, G. M. Venzor, T. J. De Lyon, J. E. Jensen, B. Z. Nosho, J. A. Roth, and J. R. Waterman, J. Electron. Mater. **33**, 517 (2004).